

Research Article

Spontaneous Magnetization in the Finite-Size Two-Leg Ising Ladder in the External Magnetic Field

Vardan Apinyan *

Department of Condensed Matter Theory, Institute of Low Temperature and Structure Research, ul. Okólna 2, Wrocław, Poland; E-Mail: v.apinyan@intibs.pl

* **Correspondence:** Vardan Apinyan; E-Mail: v.apinyan@intibs.pl

Academic Editor: Michal Nowicki

Special Issue: [New Trends in Magnetic Materials](#)

Recent Progress in Materials
2023, volume 5, issue 2
doi:10.21926/rpm.2302026

Received: March 30, 2023

Accepted: June 13, 2023

Published: June 24, 2023

Abstract

This paper considers a finite-sized two-leg ladder of spin-1/2 particles with local inter-chain Ising interaction. We include the effects of an external magnetic field by incorporating a Zeeman-type coupling between the magnetic field and the spins localized on the lattice sites. To analyze the system, we utilize the transfer-matrix formalism to calculate the partition function. We compute the magnetization for different configurations by varying the system's parameters. We observe the presence of spontaneous magnetization within the system. As the inter-chain Ising interaction changes its sign, the magnetization value changes from negative to positive values. Furthermore, we identify a phase transition from diamagnetic to ferromagnetic states when examining the temperature dependence of the magnetization at zero magnetic fields. We observe a step-like behavior in the magnetization curve in the low temperature limit.

Keywords

Spin-chains; Ising model; phase transitions; magnetic phase transitions



© 2023 by the author. This is an open access article distributed under the conditions of the [Creative Commons by Attribution License](https://creativecommons.org/licenses/by/4.0/), which permits unrestricted use, distribution, and reproduction in any medium or format, provided the original work is correctly cited.

1. Introduction

Understanding spin arrangements, spontaneous magnetization and their implementation in quasi-two-dimensional (2D) materials is important in terms of fundamental physics and technological applications [1-3]. The Ising model was useful for representing the main features of many individual systems. Lenz proposed it and solved exactly by Ising in 1925 [4]. In 1944, Lars Onsager obtained the analytical solution of the Ising model on the square lattice in the absence of the external field and by considering the nearest neighbor interactions on the lattice [5]. Furthermore, in 1950, Yang checked out Onsager's result for spontaneous magnetization and obtained the critical exponents [6]. Although the solution of the Ising model in three dimensions does not exist, one can use the Peierls argument to prove the existence of spontaneous magnetization at a sufficiently low-temperature limit [7]. It has been demonstrated that, for a quasi-two-dimensional lattice, spontaneous magnetization is equivalent to the long-range order in the system [8, 9], which proved the theory of Onsager and Yang. A rigorous proof of the spontaneous magnetization in the Ising model at finite temperatures is given in [10]. The classical Peierls argument was used for the two-dimensional lattice defined by the Sierpinski carpet fractal. Moreover, the exact result obtained there, proves the existence of spontaneous magnetization in the structures with dimensions smaller than 2.

Two-channel Ising ladders, with the inter-chain Ising interaction, were considered many years ago by R. Medjani et al. [11-13]. Nevertheless, the considered model refers only to the symmetric spin system with equal intra-chain Ising couplings in both spin chains. Spin-ladder systems got particular attention from the point of view of their experimental applicability and realization. If the inter-chain coupling is antiferromagnetic, then these models are considered high T_C materials models [14, 15]. As intermediate systems between one-dimensional and two-dimensional spin systems, the spin ladders have a diverse range and interesting quantum magnetic effects at low temperatures [16-18]. A comprehensive review of the recent advances in the thermal and magnetic properties of spin-ladder models is given in Ref. [19] regarding their applicability to the physics ladder compounds with strong coupling chains.

This paper considers a two-leg spin-1/2 ladder consisting of two chains $\ell = a, b$. The inter-chain Ising interaction is included in the calculations. By using the standard transfer- T matrix formalism, we calculate the partition function of the system. The magnetization function per-spin and per-chain was calculated from the expression of the Gibbs free energy of the system. We prove the existence of the critical value of the Ising interaction energy above which spontaneous magnetization appears in the system. Particularly, for the ferromagnetic Ising exchanges in the chains (F/F configuration), and in the low-temperature limit, the magnetization function changes drastically from 0 to 1 at some negative critical value of the inter-chains Ising coupling energy L_C . Moreover, for the case of the antiferromagnetic spin-exchange in one of the chains (F/AF configuration), the magnetization function behaves like a step-function, when varying the inter-chain Ising interaction parameter from negative to positive values. We calculate the temperature dependence of spontaneous magnetization in the system for different values of the Ising coupling parameter J_2/J_1 . We have shown that for the values $J_2/J_1 < 1$ the spontaneous magnetization takes the negative values, while, for $J_2/J_1 > 1$ the magnetization function is positive. For the symmetric case, i.e., when $J_1 = J_2$, spontaneous magnetization is absent in the system. Moreover, we obtain an unusual behavior of spontaneous magnetization as a function of the Ising interaction parameter J_2/J_1 .

The present paper is organized as follows: in Section 2 we introduce the Hamiltonian for the two-leg Ising ladder and we calculate the partition function by using \hat{T} -matrix formalism. In Section 3, we numerically the magnetization in the system and discuss the obtained results. In Section 4, we give a short conclusion to our paper.

2. Two-leg Spin System

The Hamiltonian of our model of the magnetic spin ladder, composed of two legs, each with N lattice sites, could be written in the following form

$$\hat{\mathcal{H}} = -J_1 \sum_{i=1}^N \sigma_i^a \sigma_{i+1}^a - J_2 \sum_{i=1}^N \sigma_i^b \sigma_{i+1}^b - I \sum_{i=1}^N \sigma_i^a \sigma_i^b - \mu_B H \sum_{i=1}^N \sigma_i^a - \mu_B H \sum_{i=1}^N \sigma_i^b, \quad (1)$$

where σ_i are the spin variables with the values $\sigma_i = \pm 1$ at individual lattice sites positions i , J_1 and J_2 are the two-body spin Ising interactions in the chains with $\ell = a$ for the leg a , and $\ell = b$ for the leg b . I , in Eq.(1), is Ising coupling energy between the chains and H is the uniform external magnetic field which acts to the local spins on the chains. The schematic representation of the model, discussed here, is presented in Figure 1.

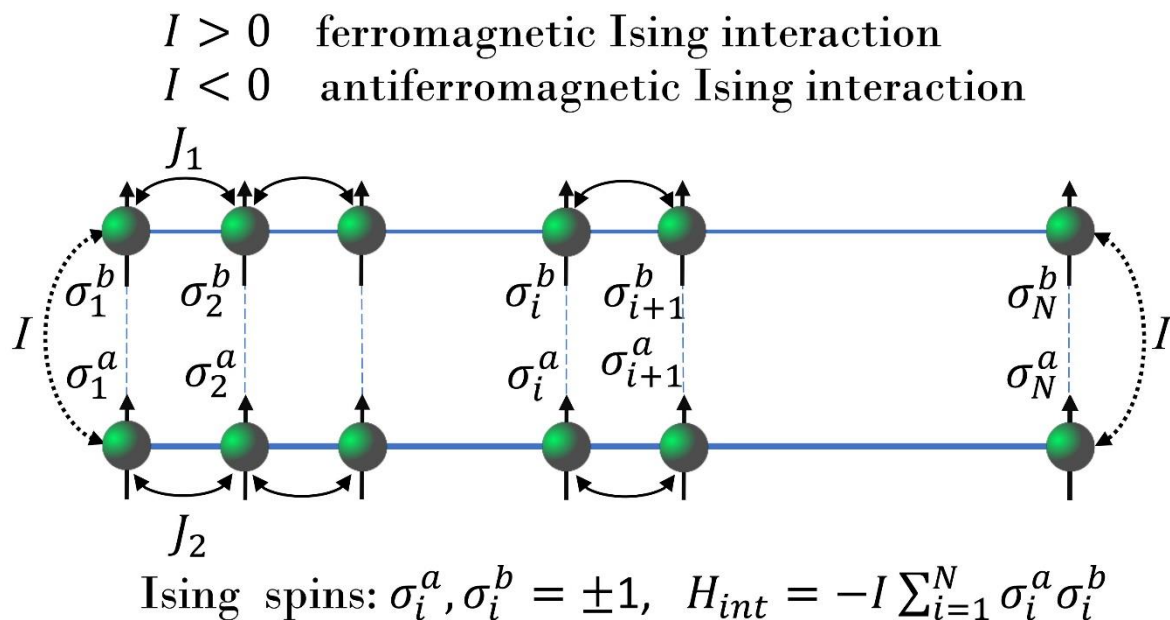


Figure 1 The schematic representation of two-leg spin systems with inter-chain Ising interaction I . The intra-chain Ising exchange energies J_1 and J_2 are shown in the picture. The sign of the Ising interaction I determines the nature of exchange correlations between the chains. Particularly, the case $I > 0$ corresponds to the ferromagnetic Ising-exchange between the chains, while the case $I < 0$ corresponds to the antiferromagnetic Ising interaction between the chains.

The partition function of the system is given as

$$\begin{aligned}
Z_N &= \sum_{\{\sigma_{i=1}^a, \sigma_{i=2}^a, \dots, \sigma_{i=N}^a = \pm 1\}} \sum_{\{\sigma_{i=1}^b, \sigma_{i=2}^b, \dots, \sigma_{i=N}^b = \pm 1\}} \exp[K_1 \sum_{i=1}^N \sigma_i^a \sigma_{i+1}^a + K_2 \sum_{i=1}^N \sigma_i^b \sigma_{i+1}^b + \\
&\quad I \sum_{i=1}^N \sigma_i^a \sigma_i^b + \frac{h}{2} \sum_{i=1}^N (\sigma_i^a \sigma_{i+1}^a) + \frac{h}{2} \sum_{i=1}^N (\sigma_i^b \sigma_{i+1}^b)] \\
&= \sum_{\left\{ \begin{array}{l} \{\sigma_{i=1}^a, \sigma_{i=2}^a, \dots, \sigma_{i=N}^a = \pm 1\} \\ \{\sigma_{i=1}^b, \sigma_{i=2}^b, \dots, \sigma_{i=N}^b = \pm 1\} \end{array} \right\}} \prod_{i=1}^N \hat{T}(\sigma_i^a \sigma_{i+1}^a, \sigma_i^b \sigma_{i+1}^b). \quad (2)
\end{aligned}$$

The constituents of the Hamiltonian in the exponent, in Eq.(2), concerning the interaction parts in Eq.(1), were written in more symmetric forms by taking into account the periodic boundary conditions on spin variables in both chains $\ell = a, b$, i.e., $\sigma_{i=1}^\ell = \sigma_{i=N+1}^\ell$. The renormalized interaction coefficients are $K_1 = J_1/k_B T$, $K_2 = J_2/k_B T$, $L = I/k_B T$ and $h = \mu_B H/k_B T$. We have introduced on the right-hand side, in Eq.(2), the transfer \hat{T} -matrix of the problem, which has the following form

$$\begin{aligned}
\hat{T}(\sigma_i^a \sigma_{i+1}^a, \sigma_i^b \sigma_{i+1}^b) &= \exp[K_1 \sum_{i=1}^N \sigma_i^a \sigma_{i+1}^a + K_2 \sum_{i=1}^N \sigma_i^b \sigma_{i+1}^b + L \sum_{i=1}^N \sigma_i^a \sigma_i^b + \\
&\quad \frac{h}{2} \sum_{i=1}^N (\sigma_i^a + \sigma_{i+1}^a) + \frac{h}{2} \sum_{i=1}^N (\sigma_i^b + \sigma_{i+1}^b)]. \quad (3)
\end{aligned}$$

Then, we calculate each element of the transfer- \hat{T} matrix, for 16 different configurations of spins on the nearest neighbors' lattice sites on different chains. We have

$$\hat{T}(\sigma_i^a \sigma_{i+1}^a, \sigma_i^b \sigma_{i+1}^b)|_{\{\sigma_i = \pm 1\}} = \begin{bmatrix} \hat{T}(\sigma_i^a = 1, \sigma_{i+1}^a = 1) & \hat{T}(\sigma_i^a = 1, \sigma_{i+1}^a = -1) \\ \hat{T}(\sigma_i^a = -1, \sigma_{i+1}^a = 1) & \hat{T}(\sigma_i^a = -1, \sigma_{i+1}^a = -1) \end{bmatrix}, \quad (4)$$

where each component of the matrix, in Eq.(4), is a 2×2 matrix. We have for each element, in Eq. (4)

$$\hat{T}(1,1) = \begin{bmatrix} e^{(K_1+K_2+L+2h)} & e^{(K_1-K_2+h)} \\ e^{(K_1-K_2+h)} & e^{(K_1+K_2+L)} \end{bmatrix}, \quad (5)$$

$$\hat{T}(1,-1) = \begin{bmatrix} e^{(-K_1+K_2+h)} & e^{(-K_1-K_2+L)} \\ e^{(-K_1-K_2-L)} & e^{(-K_1+K_2-h)} \end{bmatrix}, \quad (6)$$

$$\hat{T}(-1,1) = \begin{bmatrix} e^{(-K_1+K_2+h)} & e^{(-K_1-K_2-L)} \\ e^{(-K_1-K_2+L)} & e^{(-K_1+K_2-h)} \end{bmatrix}, \quad (7)$$

$$\hat{T}(-1,-1) = \begin{bmatrix} e^{(K_1+K_2-L)} & e^{(K_1-K_2-h)} \\ e^{(K_1-K_2-h)} & e^{(K_1+K_2+L-2h)} \end{bmatrix}. \quad (8)$$

Thus, total \hat{T} -matrix, in Eq.(4), could be rewritten in the following 4×4 form

$$\hat{T}(\sigma_i^a \sigma_{i+1}^a, \sigma_i^b \sigma_{i+1}^b)|_{\{\sigma_i = \pm 1\}} = \begin{bmatrix} e^{(K_1+K_2+L+2h)} & e^{(K_1-K_2+h)} & e^{(-K_1+K_2+h)} & e^{(-K_1-K_2+L)} \\ e^{(K_1-K_2+h)} & e^{(K_1+K_2+L)} & e^{(-K_1-K_2-L)} & e^{(-K_1+K_2-h)} \\ e^{(-K_1+K_2+h)} & e^{(-K_1-K_2-L)} & e^{(K_1+K_2-L)} & e^{(K_1-K_2-h)} \\ e^{(-K_1-K_2+L)} & e^{(-K_1+K_2-h)} & e^{(K_1-K_2-h)} & e^{(K_1+K_2+L-2h)} \end{bmatrix}. \quad (9)$$

Next, we use the expression of the partition function in Eq.(2) to calculate the Gibbs free energy per-spin. For our system composed of N interacting spins on the spin-chains, we have

$$f(T, H) = - \lim_{N \rightarrow \infty} \frac{k_B T}{N} \ln Z_N(T, H). \quad (10)$$

Next, we diagonalize the matrix in Eq.(9), and we write the partition function as a sum of its diagonal elements, i.e., the proper values of the matrix \hat{T}^N

$$Z_N(T, H) = -Sp[\hat{T}^N] = \lambda_1^N + \lambda_2^N + \lambda_3^N + \lambda_4^N. \quad (11)$$

Furthermore, the magnetization per-spin is given, as

$$m(T, H) = - \frac{\partial f(T, H)}{\partial H}. \quad (12)$$

In the next Section, we calculate, numerically, the Gibbs free energy in Eq.(10) and the magnetization function in Eq.(12) for finite-sized chains. We will consider different spin orientations in the chains and between the chains. There, we give a formula for the magnetization function, which shows the non-conventional step-like behavior, in the particular case of the Ferromagnetic/Antiferromagnetic (F/AF) Ising exchanges of spins in the chains.

Throughout the paper, we will use the units $J_1 = 1.0$ for the energy parameters in the system, and $\mu_B = 1.0$ for the magnetization function.

3. Normalized Magnetization Per-Spin, Per-Chain

The numerical calculations presented hereafter concern the magnetization of the system normalized by the number of chains, i.e., $m = M/2$, where m is the magnetization per chain. Our numerical evaluations have been done for several lattice sites equal to $N = 10^{12}$, at each chain. In Figure 2, we have presented the temperature dependence of Gibbs free energy of the system for different values of the external magnetic field. The magnetic field's influence is apparent in the ferromagnetic exchange between spins in different chains with the Ising interaction energy $L/J_1 = 1.0$. In the case of the antiferromagnetic Ising interaction with $L/J_1 = -1.0$ (see Figure 2b), the Gibbs free energy is lowered at the high magnetic field $\mu_B H/J_1 = 2.0$ (see the green curve, in Figure 2b). In Figure 3, the normalized magnetization curves have been presented as a function of temperature for the same values (see Figure 3a and Figure 3b) of the Ising interaction parameter L/J_1 , as in Figure 2. We see, in Figure 3, that the behavior of the magnetization function is completely different for different signs of the inter-chain Ising interaction parameter L/J_1 . In the case of the ferromagnetic exchange (see the curve in Figure 3a) with $L/J_1 = 1.0$ and non-zero magnetic fields, the temperature dependence of the magnetization is very similar to the usual results in 1D Ising chains. In contrast, at the zero magnetic field limit, we get the spontaneous magnetization of the system, which is absent in the traditional one-chain Ising model. Furthermore, in Figure 3b, we show the results for the antiferromagnetic exchange between the chains with $L/J_1 = -1.0$. We observe that there is a large temperature region where the magnetization increases with the temperature, attaining its maximal values at certain critical temperatures, after

which the magnetization function decreases with temperature, showing the usual behavior of the 1D Ising chain.

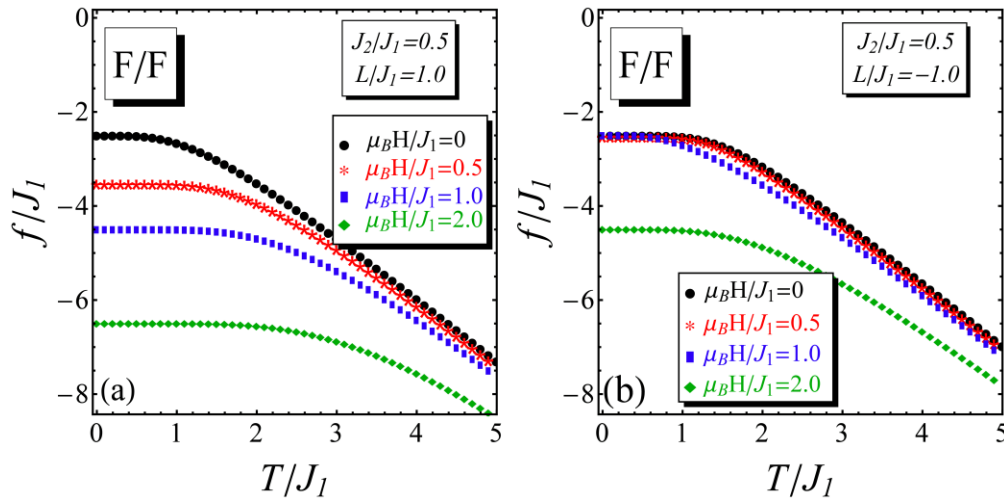


Figure 2 Gibbs free energy of the spin system composed of two chains, as a function of temperature. The following values of the Ising interaction parameters have been employed: $J_2/J_1 = 0.5$, $L/J_1 = 1.0$ (see in panel (a)) and $J_2/J_1 = 0.5$, $L/J_1 = -1.0$ (see in panel (b)). Different values (from zero up to very high) of the external magnetic field have been considered.

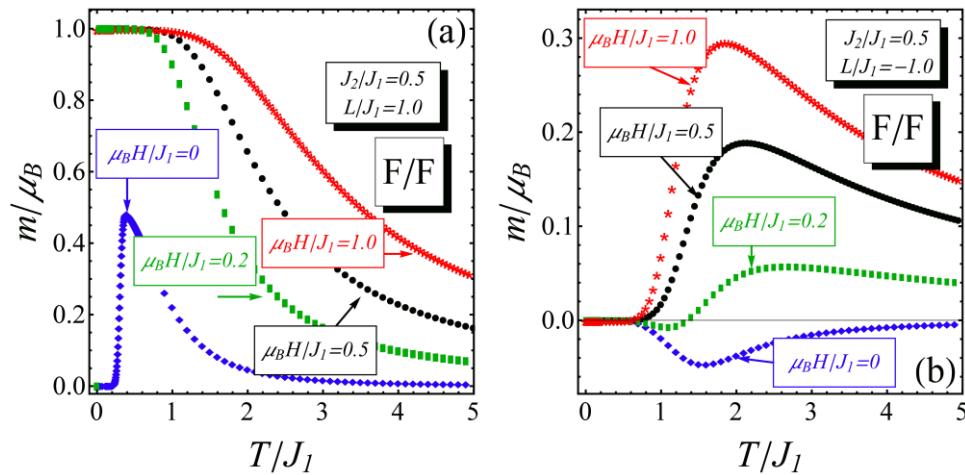


Figure 3 The magnetization of the system as a function of temperature, for different values of the external magnetic field. The ferromagnetic (F) (see in panel (a)) and antiferromagnetic (AF) (see in panel (b)) spin-exchanges between different chains have been considered during calculations.

We see that the values of those critical temperatures vary slightly with the change in the external magnetic field. Particularly, the critical temperatures are decreasing when augmenting the values of the magnetic field parameter $\mu_B H/J_1$. For non-zero magnetic fields, the numerical values of those critical temperatures T_c/J_1 could be approximated with the help of the following formula

$$T_c/J_1 = 1 + \frac{1}{(\mu_B H/J_1)^\alpha} \quad (13)$$

where α is a numerical fitting parameter that satisfies the condition $\alpha < 1$. At $\mu_B H/J_1 = 0$, we get the negative spontaneous magnetization of the system. Thus the spontaneous magnetization is nonzero and its sign is varied from positive to negative values when the sign of the inter-chain Ising interaction L/J_1 changes from positive to negative, analogously (see the blue curves in Figure 3a and 3b). We attribute the appearance of the non-zero spontaneous magnetization to the existence of the inter-chain interaction parameter L and we have calculated, in Figure 4, the dependence of the magnetization function on that parameter L , which changes from large negative to large positive values (see in Figure 4a and Figure 4b). In Figure 4a, we have shown the results for the case of the ferromagnetic-type intra-chain Ising couplings, i.e., with positive values of the parameters J_1 and J_2/J_1 . The temperature was fixed at the value $T/J_1 = 1.0$. We observe in Figure 4a, that there exists a critical value for the parameter L/J_1 ($L/J_1 = L_c/J_1$), situated in the region of the negative values of L/J_1 starting from which the magnetization appears in the system, including the spontaneous magnetization at $\mu_B H/J_1 = 0$ (see the blue curves in Figure 4). The critical values L_c/J_1 of the parameter L/J_1 vary with the change of the external magnetic field. They increase when lowering the strength of the magnetic field. When augmenting the parameter L from the value L_c/J_1 , at the fixed value of the magnetic field parameter, the magnetization per chain increases drastically and attains its maximal value equal to 1. This transition region, from 0 to 1 of the magnetization function becomes very large for the case $J_1 > 0$ and $J_2/J_1 < 0$ (see Figure 4b). The case $J_2/J_1 < 0$ corresponds to the case of the antiferromagnetic Ising interaction in the chain with $\ell = 2$. In this case, we observe also a smooth cascade-like structure of the magnetization function. Also, the negative branches of the magnetization function are absent in this case $J_2/J_1 < 0$, for both positive and negative values of the parameter L/J_1 (see Figure 4b). Meanwhile, the spontaneous magnetization of the system has only one branch solution and changes its sign with L/J_1 , in complete agreement with the results in Figure 3.

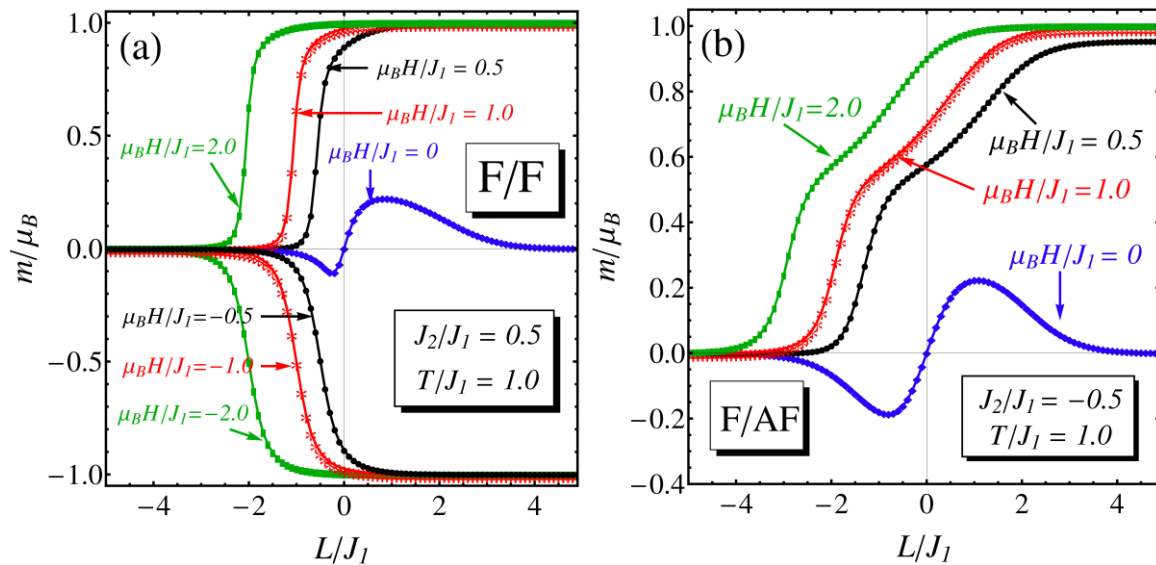


Figure 4 The magnetization of the system as a function of the inter-chain Ising interaction energy L , for different values of the external magnetic field. The Ising exchanges of spins in the legs of the ladder are of type F/F (see in panel (a)) and F/AF (see in panel (b)). The temperature is set as $T/J_1 = 1.0$.

Furthermore, within the parameter region $J_2/J_1 > 0$ when temperature decreases down to $T/J_1 = 0.5$ (see the results in Figure 5), we observe an instant magnetization jump from 0-plateau to the saturation magnetization $m = 1$ at $L/J_1 = L_c/J_1$ (see in Figure 5a). Moreover, the cascade-like behavior of the magnetization function becomes more apparent for the case $J_1 > 0$ and $J_2/J_1 < 0$. In Figure 5, we observe that the amplitudes of the spontaneous magnetization in the system drastically increase by lowering the temperature to the value $T/J_1 = 0.5$ (see blue curves plotted in Figure 5a and Figure 5b).

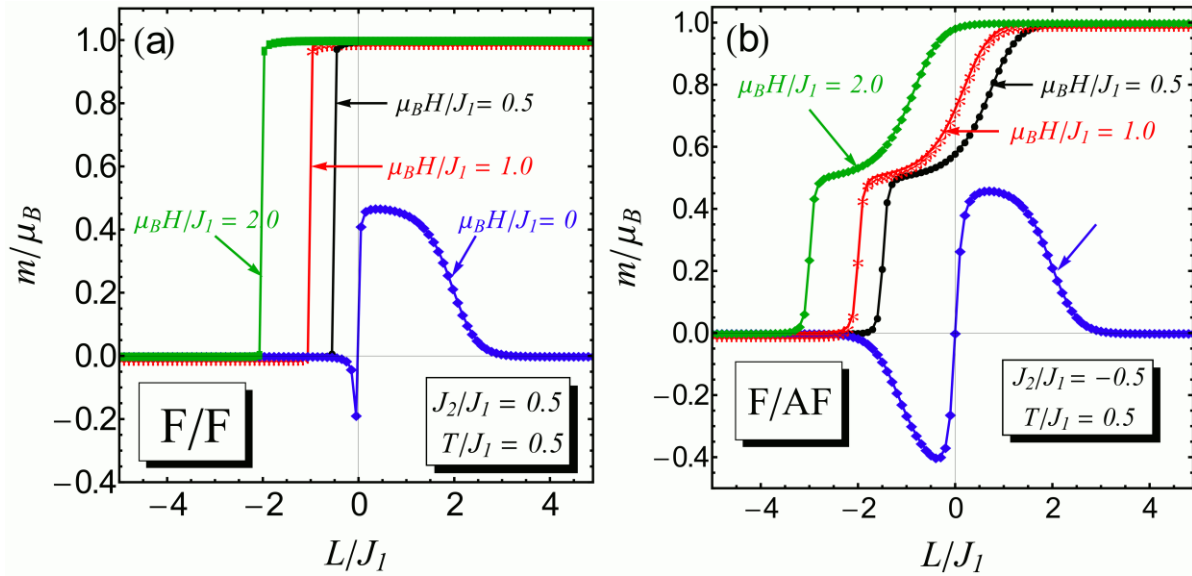


Figure 5 The magnetization of the system as a function of the inter-chain Ising interaction energy L/J_1 , for different values of the external magnetic field. The results in panel (a) have been given for the ferromagnetic spin configurations in the chains (F/F). In panel (b), we considered the F/AF-type of intra-chain spin configurations in the chains. The temperature is set as $T/J_1 = 0.5$.

From the results, obtained in Figure 5, we can conclude that the two-leg spin system behaves like a two-level model with the magnetization equal to $m = 0$, for $L/J_1 < L_c/J_1$ and $m = 1.0$, for $L/J_1 \geq L_c/J_1$, i.e.,

$$m = m_0 \theta(L/J_1 - L_c/J_1) \quad (14)$$

with $m_0 = 1$ and $\theta(x)$ being the Heaviside step function. We also observe that the critical values L_c/J_1 , obtained for the inter-chain Ising interaction parameter, could be approximated with the help of the formula

$$L_c = -\frac{\mu_B H}{2J_2} \quad (15)$$

at $\mu_B H/J_1 \neq 0$. Indeed, the critical values of the inter-chain Ising interaction appear only at the low-temperature regime ($0 < T/J_1 < 0.5$), and the magnetization function jumps from zero to the finite values (see Figure 5a), while for high temperatures the curves get smoothed. Their is no

sense to speak about critical values. In the interval $0 < T/J_1 < 0.5$, the critical values L_c remain unchanged.

Furthermore, in Figure 6, we give the results for the magnetization function at the relatively low-temperature case with $T/J_1 = 0.1$ and for different values of the magnetic field parameter $\mu_B H/J_1$. The Ising couplings in the chains have been fixed at the values $J_1 = 1.0$ and $J_2/J_1 = -0.5$, corresponding to the case of the ferromagnetic and antiferromagnetic exchanges in the chains with $\ell = 1$ and $\ell = 2$, respectively. We obtain the step-like multilevel behavior of the magnetization function

$$m = \begin{cases} m_{0.5}\theta(L/J_1 - L_1/J_1), & \text{if } L/J_1 \in (0, L_1/J_1) \\ m_{0.5} + m_{0.5}\theta(L/J_1 - L_2/J_1), & \text{if } L/J_1 \in (0, L_2/J_1) \\ m_{1.0} + m_{0.5}\theta(L/J_1 - L_3/J_1), & \text{if } L/J_1 > L_3/J_1. \end{cases} \quad (16)$$

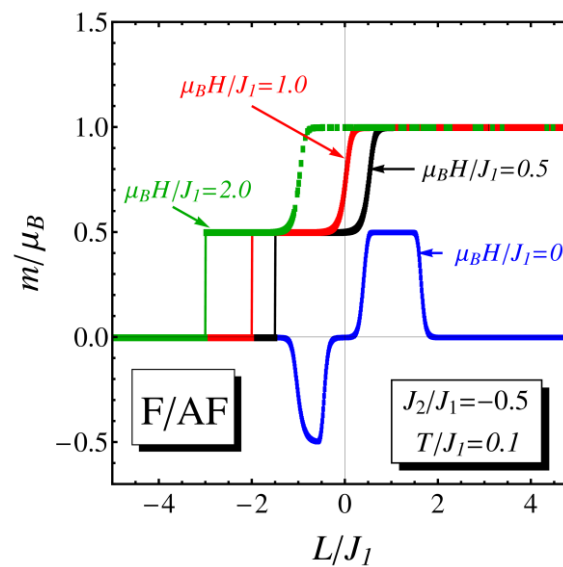


Figure 6 The magnetization of the system as a function of the inter-chain Ising interaction energy L/J_1 , for different values of the external magnetic field. The results are given for the F/AF-type spin configuration in the magnetic chains. The temperature is set as $T/J_1 = 1.0$.

Here, $m_{0.5} = 0.5$.

Where $m_{0.5} = 0.5$, and $m_1 = 1.0$. Such a step-like behavior of the magnetization function has been observed in Ref. [20], in the strong antiferromagnetic rung coupling regime, where the saturation magnetization plateau has been observed by using the Thermodynamic Bethe Ansatz approach.

In Figure 7 and Figure 8, we have shown the field dependence of the magnetization function for different values of the inter-chain Ising interaction parameter L/J_1 . The behavior of curves is practically the same as in the case of the 1D Ising model, except the case corresponding to the negative value of the inter-chain interaction energy, i.e., $L/J_1 = -1.0$ (see red curves in Figure 7 and Figure 8). Particularly, for the magnetic field smaller than the saturation field, the magnetization, at the given value of the magnetic field $\mu_B H/J_1 = \mu_B H_0/J_1$, is larger for the case of ferromagnetic inter-chain interaction (see black curves in Figure 7, when $L/J_1 = 1.0$). We also observe that for the case $J_2/J_1 = -0.5$ (see in Figure 7b, and Figure 8b) there exists a negative spontaneous

magnetization at zero value of the magnetic field, for $L/J_1 = -1.0$ (see red curves in Figure 7b, and Figure 8b).

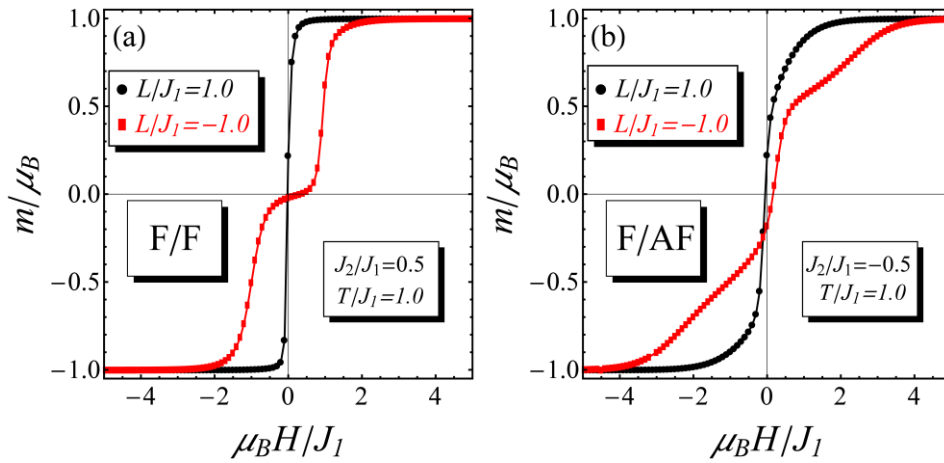


Figure 7 The field dependence of the magnetization in the system, for two different values of the inter-chain Ising interaction parameter L/J_1 . In panel (a), we considered ferromagnetic Ising couplings F/F in the chains. In panel (b), spins interact ferromagnetically in the chain with $\ell = 1$ and antiferromagnetically in the chain with $\ell = 2$. The temperature is set as $T/J_1 = 1.0$.

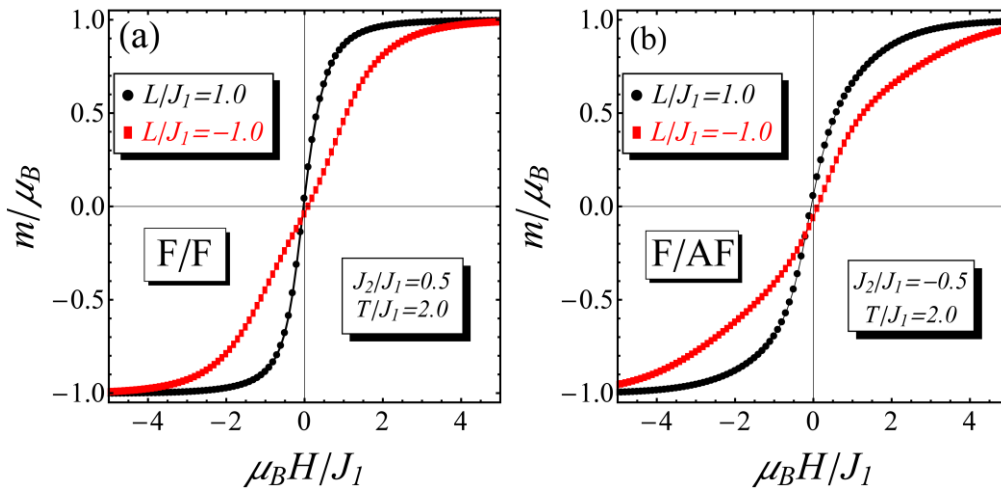


Figure 8 The field dependence of the magnetization in the system, for two different values of the inter-chain Ising interaction parameter L/J_1 . In panel (a), we considered ferromagnetic Ising couplings F/F in the magnetic chains. In panel (b), spins interact ferromagnetically in the chain with $\ell = 1$ and antiferromagnetically in the chain with $\ell = 2$. The temperature is set as $T/J_1 = 2.0$.

The curves of the magnetization function, for the case $J_2/J_1 > 0$ (see in Figure 7a) and Figure 8a, are symmetric concerning the magnetic field axis with a reflection to the negative values of the normalized magnetic field parameter $\mu_B H/J_1$. This is true for both ferromagnetic and antiferromagnetic Ising interactions between ladders. Meanwhile, this symmetry gets destroyed when $J_2/J_1 < 0$, and a finite magnetization appears at $\mu_B H/J_1 = 0$. The reason is related to the strong antiferromagnetic fluctuations in this last case. It is worth mentioning here that the behavior

of the magnetization function in the case of the antiferromagnetic Ising interaction between the chains, given in Figure 7a, (see the red curve on the picture) corresponds well to the behavior of the magnetization for the strong coupling ladder compound $(5IAP)_2CuBr_4 \cdot 2H_2O$, and discussed in Refs. [19] and [21].

In Figure 9, we have shown the temperature dependence of the spontaneous magnetization in the system ($\mu_B H/J_1 = 0$) for different positive values of the Ising coupling parameter J_2/J_1 in the chain with $\ell = 2$. The magnetic field is set at zero and the Ising coupling parameter J_1 was fixed at the value $J_1 = 1.0$. We considered the antiferromagnetic exchange between the chains with the inter-chain interaction energy $L/J_1 = -1.0$. This corresponds to the antiparallel orientations of spins between the chains. We see in Figure 9a and Figure 9b that when $J_2/J_1 < 1$, the spontaneous magnetization of the system is negative. For $J_2/J_1 = 1.0$, which corresponds to the symmetric case $J_1 = J_2$ we have $m = 0$ (this is not shown in the picture). Thus, for the symmetric coupling in the chains, i.e., when $J_1 = J_2$, the spontaneous magnetization is absent; nevertheless, the inter-chain interaction is not zero (this result is equivalent to the usual 1D Ising model). For the values $J_2/J_1 > 1.0$, the spontaneous magnetization becomes positive. Moreover, we observe in Figure 9 that the magnetization continuously increases upon increasing the interaction ratio J_2/J_1 , from $J_2/J_1 = 0$ to the value $J_2/J_1 = 2.0$. The negative values of the magnetization function in Figure 9a could be explained as the states of possible diamagnetism in the two-leg system ($m/\mu_B < 0$). When $m/\mu_B = 0$, at $J_1 = J_2$, the system is nonmagnetic. Thus it is in the insulating regime, and when $J_2/J_1 > 0$, the system has positive magnetization, thus by representing a ferromagnetic state. Therefore, we can conclude that the relative values and signs of Ising exchange parameters J_1 and J_2 determine different possible phases in the two-leg system considered here. That exceptional behavior could be extremely important for such two-ladder constructions' experimental setups and technological applications.

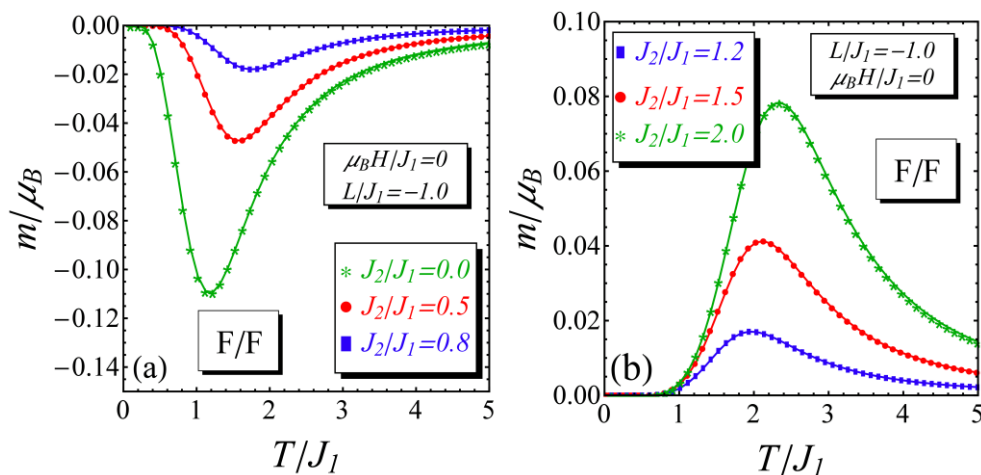


Figure 9 The normalized spontaneous magnetization of the system as a function of temperature, for different values of the exchange energy parameter J_2/J_1 . We have considered the antiferromagnetic Ising interaction between the chains with the interaction parameter $L/J_1 = -1.0$, and the spins interact ferromagnetically in the chain with $\ell = 1$.

In Figure 10, the field dependence of Gibbs free energy function is presented, for different values of the inter-chain Ising interaction parameter L/J_1 and different values of the parameter J_2/J_1 . A

sufficiently low-temperature limit is considered with $T/J_1 = 0.2$. We see, in Figure 10, that, for the case of F/F spin junction and for $L/J_1 = -1.0$, a region of constant-energy plateau appears for a large interval of variation of the magnetic field parameter B . Particularly, $f/J_1 = -2.5$ for $H \in [-1.0, 1.0]$ (see the red curve, in Figure 10a). In Figure 11, the spontaneous magnetization is shown as a function of the Ising coupling parameter J_2/J_1 for two different values of the Ising interaction energy L/J_1 . The temperature was fixed at the value $T/J_1 = 1.0$.

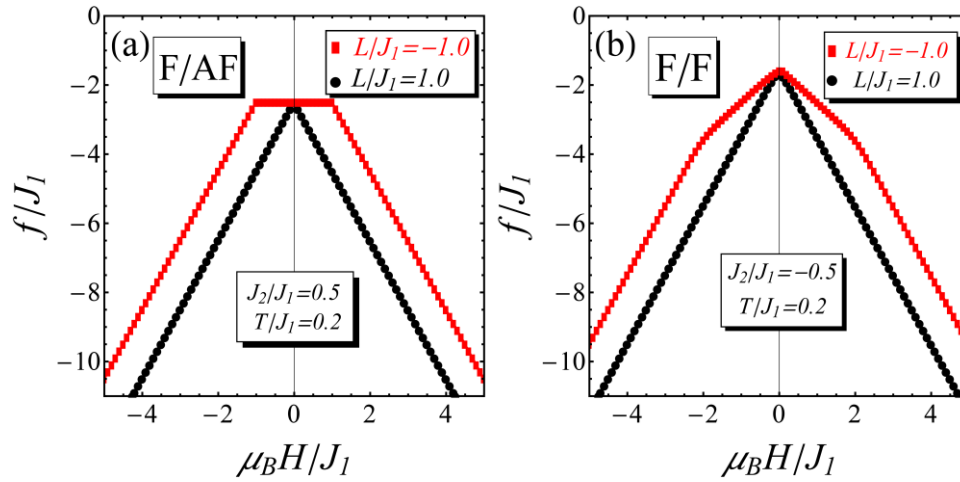


Figure 10 The field-dependence of Gibbs free energy, for different values of the inter-chain Ising interaction parameter L/J_1 . In panel (a), we considered the positive values of the interaction parameters J_1 and J_2/J_1 , which corresponds to the ferromagnetic orientations of spin in the chains. In panel (b), the spins interact ferromagnetically in the chain with $\ell = 1$ and antiferromagnetically, in the chain with $\ell = 2$. The temperature is set as $T/J_1 = 0.2$.

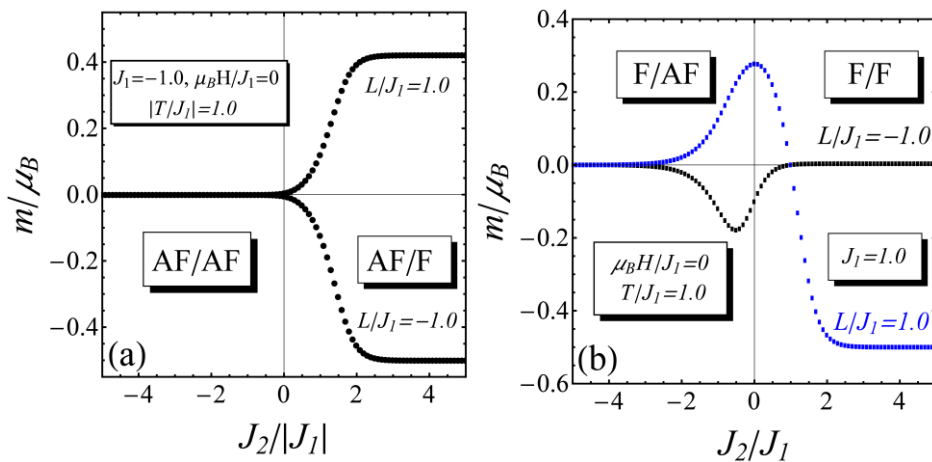


Figure 11 The normalized spontaneous magnetization of the system as a function of Ising coupling energy parameter J_2/J_1 . Two different values of the exchange parameter L/J_1 , were considered. In panel (a), we examined the antiferromagnetic Ising exchange of spins in the leg with $\ell = 1$ and the parameter J_1 is set at the value $J_1 = -1.0$. In panel (b), the ferromagnetic spin-exchange was considered in the leg with $\ell = 1$, and the parameter J_1 is set at the value $J_1 = 1.0$. The temperature is set as $T/J_1 = 1.0$.

Moreover, in Figure 11a, we have fixed the parameter J_1 at the value $J_1 = -1.0$. Thus, when $J_2/|J_1| < 0$, we have the region of antiferromagnetically ordered spins in both chains (this is the region AF/AF) and the spontaneous magnetization is zero. Thus the spin ladder system is in the insulating regime. In the semi-plane with $J_2/|J_1| > 0$, we have antiferromagnetic spin ordering in the chain with $\ell = a$, and ferromagnetic spin ordering in the chain with $\ell = b$. This region is represented as AF/F, in Figure 11a. We get nearly symmetric behavior of the magnetization function, with respect to the J_2/J_1 -axis. The reason for this antisymmetric is described by the change of the sign of the inter-chain Ising interaction parameter L/J_1 , namely, when $L/J_1 < 0$ we have the spin ladder system in the diamagnetic state with $m/\mu_B < 0$. In Figure 11b, we considered the ferromagnetic spin-exchange in the chain with $\ell = 1$.

In the region $J_2/J_1 < 0$, we have the ferromagnetic Ising exchange in the chain $\ell = 1$ and antiferromagnetic Ising exchange in the chain $\ell = 2$. This region is represented as F/AF, in Figure 11b. In the semi-plane with $J_2/J_1 > 0$ we have the ferromagnetic Ising exchange in both chains and this region is represented as F/F in Figure 11b. For ferromagnetic case $J_1 > 0$, the spontaneous magnetization is nonzero in the regions $J_2/J_1 < 0$ and $J_2/J_1 > 0$, which is in contrast to the antiferromagnetic case $J_1 < 0$, considered in Figure 11a.

4. Concluding Remarks

In this paper, we considered, theoretically, the two-leg spin ladder with the local inter-chain Ising interaction. The magnetic field is included in the calculations by coupling with the individual spin variables. By employing the \hat{T} -matrix approach, we calculated the Gibbs free energy of such a system and the magnetization function for different values of the Ising terms in the chains and inter-chains. The calculations show the appearance of spontaneous magnetization in the system for the appropriate regime of the interaction parameters. For the ferromagnetic spin exchange in the legs and the inter-chain Ising interaction, the magnetization shows the usual behavior as a function of temperature, typical to the 1D Ising model. The differences appear in the case of the antiferromagnetic inter-chain Ising interaction. In this case, we obtain a critical temperature T_c/J_1 , such that for $T/J_1 < T_c/J_1$ the magnetization is zero and for $T/J_1 > T_c/J_1$ there is a non-zero magnetization in the system. We have found the critical value L_c/J_1 of the inter-chain Ising interaction parameter above which the magnetic phase transition appears in the system. We have shown that in the low-temperature regimes, and for the F/F intra-chain spin-configuration, the system is typical of two-level systems with $m(L < L_c) = 0$ and $m(L > L_c) = 0$. Meanwhile, for the F/AF configuration of spins in the chains, the magnetization has a step-like cascade behavior as a function of the inter-chain Ising interaction parameter L/J_1 . For the case of the antiferromagnetic inter-chain interaction ($L/J_1 < 0$) and symmetric spin-arrangement in the chains, i.e., $J_1 = J_2 > 0$, the magnetization of the system is zero, while for the case $J_1 \neq J_2$ the magnetization $m(T)$ changes its sign as a function of the interaction parameter J_2/J_1 . Particularly, for the case, $J_1 = 1.0$ and $J_2/J_1 < 1.0$ the magnetization is negative $m(T) < 0$, while, for $J_2/J_1 > 1.0$, the spontaneous magnetization takes the positive values $m(T) > 0$. Thus, depending on the value of the Ising coupling parameter in one of the chains (here, the parameter J_2/J_1), the phase transition occurs in the system, from the diamagnetic to the ferromagnetic states.

The results obtained in the paper could be stimulating to consider the two-leg spin ladder as one of the candidates for its applications as a quasi-two-dimensional model where spontaneous

magnetization exists. Concerning the behavior of the magnetization function in the low-temperature limit, the two-leg spin ladder could be regarded as a two-level system, which also opens the possibilities for its use in the new quantum technologies and quantum information theories.

Concerning the behavior of the magnetization function in the low-temperature limit, the two-leg spin ladder could be considered as a two-level system, which also opens the possibilities for its use in the new quantum technologies and quantum information theories.

Author Contributions

The author did all the research work of this study.

Competing Interests

The author has declared that no competing interests exist.

References

1. Dagotto E, Rice TM. Surprises on the way from one- to two-dimensional quantum magnets: The ladder materials. *Science*. 1996; 271: 618.
2. Hutak T, Krokhmalskii T, Rojas O, de Souza SM, Derzhko O. Low-temperature thermodynamics of the two-leg ladder Ising model with trimer rungs: A mystery explained. *Phys Lett A*. 2021; 387: 127020.
3. Arian Zad H, Ananikian N. Enhanced magnetocaloric effect in a mixed spin-(1/2, 1) Ising–Heisenberg two-leg ladder with strong–rung interaction. *Eur Phys J Plus*. 2021; 136: 597.
4. Brush SG. History of the Lenz-Ising model. *Rev Mod Phys*. 1967; 39: 883.
5. Onsager L. Crystal statistics. I. A two-dimensional model with an order-disorder transition. *Phys Rev*. 1944; 65: 117.
6. Yang CN. The spontaneous magnetization of a two-dimensional Ising model. *Phys Rev*. 1952; 85: 808.
7. Bonati C. The Peierls argument for higher dimensional Ising models. *Eur J Phys*. 2014; 35: 035002.
8. Martin-Löf A. On the spontaneous magnetization in the Ising model. *Commun Math Phys*. 1972; 24: 253.
9. Montroll EW, Potts RB, Ward JC. Correlations and spontaneous magnetization of the two-dimensional Ising model. *J Math Phys*. 1963; 4: 308.
10. Vezzani A. Spontaneous magnetization of the Ising model on the Sierpinski carpet fractal, a rigorous result. *J Phys A*. 2003; 36: 1593.
11. Mejdani R, Lambros A. Ladder Ising spin configurations. I. Heat capacity. *Phys Status Solidi*. 1996; 196: 433-441.
12. Mejdani R, Gashi A, Ciftja O, Lambros A. Ladders with two, three and four coupled Ising spin chains. magnetic properties. Trieste: International centre for theoretical physics; 1995.
13. Mejdani R, Gashi A, Ciftja O, Lambros A. Ladder Ising spin configurations II. magnetic properties. *Phys Status Solidi*. 1996; 197: 153-164.

14. Dagotto E, Riera J, Scalapino D. Superconductivity in ladders and coupled planes. *Phys Rev B*. 1992; 45: 5744.
15. Sigrist M, Rice TM, Zhang FC. Superconductivity in a quasi-one-dimensional spin liquid. *Phys Rev B*. 1994; 49: 12058-12061.
16. Dagotto E, Rice TM. Surprises on the way from one-to two-dimensional quantum magnets: The ladder materials. *Science*. 1996; 271: 618-623.
17. Dagotto E. Experiments on ladders reveal a complex interplay between a spin-gapped normal state and superconductivity. *Rep Prog Phys*. 1999; 62: 1525.
18. Diep HT. *Frustrated spin systems*. 2nd ed. Singapore: World scientific; 2013.
19. Batchelor MT, Guan XW, Oelkers N, Tsuboi Z. Integrable models and quantum spin ladders: Comparison between theory and experiment for the strong coupling ladder compounds. *Adv Phys*. 2007; 56: 465-543.
20. Batchelor MT, Guan XW, Oelkers N, Ying ZJ. Quantum phase diagram of an exactly solved mixed spin ladder. *J Stat Phys*. 2004; 116: 571-589.
21. Landee CP, Turnbull MM, Galeriu C, Giantsidis J, Woodward FM. Magnetic properties of a molecular-based spin-ladder system: $(5\text{IAP})_2\text{CuBr}_4 \cdot 2\text{H}_2\text{O}$. *Phys Rev B*. 2001; 63: 100402.